Hexagonal-based ordered phases in H-Zr

Laurent Holliger,* Alexandre Legris,† and Rémy Besson‡
Laboratoire de Métallurgie Physique et Génie des Matériaux, CNRS UMR 8517, Université des Sciences et Technologies de Lille, Bâtiment C6, 59655 Villeneuve d'Ascq Cedex, France

(Received 23 March 2009; revised manuscript received 2 September 2009; published 25 September 2009)

Recent research has shown the possible presence of α-based hydride superstructures in the two-phase α-δ equilibrium region of H-Zr. This evidences the relevance of investigating the coherent phase diagram at the atomic scale, a task performed in this paper using a combination of cluster expansion (CE) and electronic structure methods. Our work points out the existence of various metastable ordered structures, some of them CE predicted and confirmed by the *ab initio* calculations, and shows the H-Zr system as conveniently described by CEs not exceeding fourth-neighbor interactions. Apart from second-order long-range interactions parallel to the c axis, these interactions stabilize these hydrides as stackings of "H biplanes" parallel to the basal plane.

DOI: 10.1103/PhysRevB.80.094111 PACS number(s): 61.66.Dk, 64.60.De, 64.70.kd

I. INTRODUCTION

Hydrogen in metals constitutes an issue focusing vast scientific efforts devoted to the search of new energy supplies.[1] In the case of zirconium, an additional technological interest arises from the use of Zr alloys[2] in nuclear industry, essentially as cladding materials submitted to corrosion phenomena producing important amounts of hydrogen. The absorption of H by the metal and the subsequent hydride precipitation may lead to significant embrittlement, depending on the hydride distribution and the thermodynamic conditions. Understanding the mechanisms of hydride formation is therefore an important safety issue, as well as a fundamental one, involving different stable and metastable hydride phases,[3] the influence of which is still poorly known. At moderate temperature, the equilibrium phase diagram is rather simple in the 0 (Zr) to 2/3 (ZrH_2) domain of H atomic fraction: phase separation should occur between an α Zr(H) solid solution with low H content and a ZrH_{2-x} ($x \simeq 0.4$) δ phase with fluorine (CaF_2) structure. For higher H amounts, a nearly stoichiometric bct ("body-centered tetragonal," $c/a<1$) ZrH_2 ϵ compound appears, in equilibrium with δ. In addition, a metastable γ phase ("face-centered tetragonal," $c/a>1$) with composition close to ZrH is often experimentally observed after quenching. More recently, a new ordered compound (called ζ) fully coherent with α Zr was detected, with a composition close to Zr_2H.[4] γ being the most frequently studied phase, a question arises about the nature of the early stages of its precipitation, which may involve coherent clusters either of type ZrH (Ref. 5) (henceforth called γ') or ζ.[4] TEM observations show that both the ζ and γ precipitates show characteristic morphologies, with needles parallel to the basal plane of the hexagonal lattice and aligned along the compact crystallographic directions.

These observations emphasize the relevance of studying properties of the coherent Zr-H system on a hexagonal lattice. To this aim, cluster expansion (CE) methods are currently the best theoretical tool for the atomic-scale study of thermodynamic properties in condensed-matter science,[6,7] including both stable and metastable systems. When using these methods, two major difficulties, however, arise: (i) the reliable determination of those relevant clusters to be taken into account, (ii) the numerical assessment of the corresponding energy coefficients. Such limitations have been partly overcome during the last decade through the introduction of statistical procedures, enabling to optimize the selection of clusters that enter in a CE, coupled with atomic-scale electronic structure calculations. These elements have turned these cluster-based configurational energetic descriptions into better predictive tools for equilibrium thermodynamic calculations,[7] and more recently to describe kinetic processes in alloys.[8] Finally, the interest of studying the H-Zr system is raised further by the fact that CE methods have scarcely been applied to hexagonal systems.[9] The present work is organized as follows: the underlying methodology is described in Sec. II, the CE elaboration and resulting low-temperature (low-T) properties are investigated in Sec. III, and Sec. IV uses this CE modeling to infer hydride properties at moderate temperatures (500 K).

II. METHODS

A. Clusters in the H-Zr system

In the present investigation of H-Zr properties, the Zr sublattice (reasonably supposed to be vacancy free and inaccessible to H atoms) was not taken into account in the CE modeling, hence a pseudobinary model including H atoms and "vacancies," both located on the tetrahedral[10] sublattice (Fig. 1). Such an implicit treatment of inert species is widespread in configurational thermodynamics of nonmetallic—especially ionic—systems [for instance, oxides (Ref. 11)]. Within the CE framework, the energy can be written quite generally as a function of the configuration:

$$E(c) = \sum_{\alpha, I_\alpha} J^\alpha_{I_\alpha} p^\alpha_{I_\alpha}(c), \tag{1}$$

where the coefficients $J^\alpha_{I_\alpha}$ are the (unknown) cluster-energy coefficients, and $p^\alpha_{I_\alpha}(c)$ are cluster "chemical indicators." It has been shown that the latter can be chosen in various ways[6,12] (including different forms of polynomials), designed to provide eventually more tractable formalisms for subsequent applications in analytical schemes, such as the cluster variation method (CVM). In the present case, since no CVM

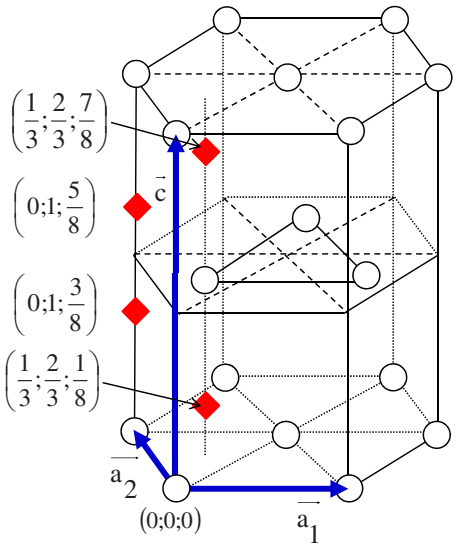

FIG. 1. (Color online) Interstitial sites in the α H-Zr structure. The spheres (resp. diamonds) represent zirconium atoms (resp. tetrahedral interstitial sites).

developments were intended for H-Zr, we adopted a lighter and equivalent choice, simply defining $p^{\alpha}_{I_{\alpha}}(c)$ as products (over each cluster) of site indicators, that take the value 1 if the cluster α has chemistry I_{α}, 0 otherwise. Since the emergence of accurate *ab initio* methods for energy calculations, the coefficients $J^{\alpha}_{I_{\alpha}}$ are now currently fitted on the energies of structures calculated *ab initio*, an approach followed in the present work. The symmetry of the underlying crystal permits to greatly reduce the number of coefficients by assigning equal values to the $J^{\alpha}_{I_{\alpha}}$ of symmetry-related clusters.[13]

A critical issue when constructing CEs is the necessarily finite range of the interactions (CE truncation), which may lead to a reduced predictive accuracy when long-range elastic effects are important. In particular, it has been shown that the properties of multilayered substitutional solutions involving size-mismatched atoms can be more adequately modeled by introducing so-called "mixed-basis" (MB) CEs (see, for instance, Ref. 14), in which the pair part of the CE is reformulated in reciprocal space, as a sum over $\vec{k}$ wave vectors in the Brillouin zone. Although the MBCE formalism, in principle, therefore enables to take into account pair interactions with arbitrary distance, its efficiency critically depends on the treatment of the long wavelengths terms ("$k=0$ singularity"),[15] which requires to get a precise enough picture of the relevant k values around the origin of the Brillouin zone. This is practically achieved by the preliminary evaluation, from continuum elasticity arguments, of a "constituent strain energy," then subtracted from each *ab initio* energy in the structure set before the MBCE is finally fitted on the corrected energies. While this procedure was shown to yield improved results in presence of sharp heterophase interfaces within substitutional solutions, it has not been extended to interstitial systems. Since we are primarily concerned here with bulk thermodynamics of H-Zr (for which such interfacial effects are probably less important), and elasticity is partially accounted for by the atomic relaxations of the input *ab initio* structures, the present approach will be restricted to "real-space" short-range (nonreciprocal) CEs, leaving for future works any further treatment of elastic effects. Indeed, in the case of H-Zr, owing to the significant relative lattice expansion of the limiting coherent phase ZrH_2 with respect to α Zr (2% in the basal plane and 15% along the c axis), such refined treatments of the elastic effects may be valuable, especially when investigating the formation of coherent vs incoherent precipitates [as already evidenced in other systems such as Al-Zn (Ref. 16)], a task, however, far beyond the scope of the present work.

TABLE I. Number of clusters (excluding ∅ and •) within each R^p_n family for the α H-Zr system.

	Number of sites, p						
Range, n	2	3	4	5	6	7	8
2	1						
2	2						
3	3	4					
4	4	10	14	15			
5	5	15	28	35	39	40	
6	6	17	33	43	50	52	53

As previously stated, only a limited number of multisite clusters can be used practically, and approximations on the range (R) and on the number of sites (p) of a cluster must therefore be introduced. Following the classification of clusters proposed in Ref. 17 for cubic materials, the range will refer throughout to the neighbor shells in the tetrahedral sublattice, with R^p_n the ensemble of clusters containing at most p sites separated of each other by at most the nth neighbor distance. The interest of such a classification stems from the fact that increasing both parameters leads to an exact expression for the energy.[6] Table I displays the number of clusters for the families of the H-Zr system up to $n=8$ and $p=6$. The cluster coordinates (up to triplets) are referenced in Table II.

The exponentially increasing number of cluster combinations with (n,p) prevents from selecting relevant clusters via an exhaustive search on R^p_n. Two routes can be followed to overcome this difficulty: either using heuristic minimization schemes [Monte Carlo (MC) or genetic algorithms[18]], or by performing an exhaustive search on a restricted ensemble of CEs built from R^p_n. In this work, the second approach was chosen with the invariant cluster expansion (ICE) approximation. Under this assumption, introduced[19] and partly justified[12] by previous works, including a cluster implies to retain all its subclusters. For some systems,[17] ICEs have been found to converge more rapidly with (n,p) than noninvariant ones. Table III indicates the number of ICEs for each family. Due to computational limitations, the present study was restricted to R^4_6, namely, to quadruplets and to the sixth neighbor shell. In this context, instead of a total number of ICEs equal to 2^{34}, the largest number of candidate CEs that have to be handled in the present work is reduced to 346 747 for R^4_6.

B. Fitting of H-Zr energetics

The next step, after building clusters and ICEs, consists in choosing the set of structures for the CV fitting procedure.

TABLE II. Cluster site coordinates for optimal CEs of R_3-R_6 (Rx=neighbor range, the last figure distinguishes between clusters of same range and number of sites).

Point		$(\frac{2}{3}\ \frac{1}{3}\ \frac{1}{8})$			
Pairs	PR1	$(\frac{2}{3}\ \frac{1}{3}\ \frac{1}{8})$	$(\frac{2}{3}\ \frac{1}{3}\ \frac{3}{8})$		
	PR2	$(\frac{2}{3}\ \frac{1}{3}\ \frac{1}{8})$	$(\frac{1}{3}\ -\frac{1}{3}\ -\frac{1}{8})$		
	PR3	$(\frac{2}{3}\ \frac{1}{3}\ \frac{1}{8})$	$(\frac{1}{3}\ -\frac{1}{3}\ -\frac{3}{8})$		
	PR4	$(\frac{2}{3}\ \frac{1}{3}\ \frac{1}{8})$	$(\frac{2}{3}\ -\frac{2}{3}\ \frac{1}{8})$		
	PR5	$(\frac{2}{3}\ \frac{1}{3}\ \frac{1}{8})$	$(\frac{2}{3}\ -\frac{2}{3}\ \frac{3}{8})$		
	PR6	$(\frac{2}{3}\ \frac{1}{3}\ \frac{1}{8})$	$(\frac{2}{3}\ \frac{1}{3}\ -\frac{5}{8})$		
Triplets	TR3	$(\frac{2}{3}\ \frac{1}{3}\ \frac{1}{8})$	$(\frac{2}{3}\ \frac{1}{3}\ \frac{3}{8})$	$(\frac{1}{3}\ -\frac{1}{3}\ -\frac{1}{8})$	
	TR41	$(\frac{2}{3}\ \frac{1}{3}\ \frac{1}{8})$	$(\frac{5}{3}\ \frac{1}{3}\ \frac{1}{8})$	$(\frac{2}{3}\ -\frac{2}{3}\ \frac{1}{8})$	
	TR43	$(\frac{2}{3}\ \frac{1}{3}\ \frac{1}{8})$	$(\frac{4}{3}\ \frac{2}{3}\ -\frac{1}{8})$	$(\frac{1}{3}\ -\frac{1}{3}\ -\frac{1}{8})$	
	TR44	$(\frac{2}{3}\ \frac{1}{3}\ \frac{1}{8})$	$(\frac{4}{3}\ \frac{2}{3}\ \frac{5}{8})$	$(\frac{1}{3}\ -\frac{1}{3}\ \frac{5}{8})$	
	TR45	$(\frac{2}{3}\ \frac{1}{3}\ \frac{1}{8})$	$(\frac{2}{3}\ \frac{4}{3}\ \frac{1}{8})$	$(-\frac{1}{3}\ \frac{1}{3}\ \frac{1}{8})$	
	TR52	$(\frac{2}{3}\ \frac{1}{3}\ \frac{1}{8})$	$(\frac{1}{3}\ \frac{2}{3}\ -\frac{1}{8})$	$(\frac{1}{3}\ -\frac{1}{3}\ -\frac{3}{8})$	
	TR53	$(\frac{2}{3}\ \frac{1}{3}\ \frac{1}{8})$	$(\frac{2}{3}\ \frac{1}{3}\ \frac{3}{8})$	$(-\frac{1}{3}\ -\frac{2}{3}\ \frac{1}{8})$	
	TR54	$(\frac{2}{3}\ \frac{1}{3}\ \frac{1}{8})$	$(\frac{2}{3}\ \frac{4}{3}\ \frac{3}{8})$	$(-\frac{1}{3}\ \frac{1}{3}\ \frac{1}{8})$	
	TR61	$(\frac{2}{3}\ \frac{1}{3}\ \frac{1}{8})$	$(\frac{4}{3}\ \frac{2}{3}\ \frac{5}{8})$	$(\frac{4}{3}\ \frac{2}{3}\ -\frac{1}{8})$	
Quadruplets	QR42	$(\frac{2}{3}\ \frac{1}{3}\ \frac{1}{8})$	$(\frac{1}{3}\ \frac{2}{3}\ \frac{5}{8})$	$(\frac{4}{3}\ \frac{2}{3}\ \frac{5}{8})$	$(\frac{1}{3}\ -\frac{1}{3}\ \frac{5}{8})$
	QR44	$(\frac{2}{3}\ \frac{1}{3}\ \frac{1}{8})$	$(\frac{1}{3}\ \frac{2}{3}\ -\frac{1}{8})$	$(\frac{2}{3}\ \frac{1}{3}\ \frac{3}{8})$	$(\frac{1}{3}\ -\frac{1}{3}\ -\frac{1}{8})$
	QR51	$(\frac{2}{3}\ \frac{1}{3}\ \frac{1}{8})$	$(-\frac{1}{3}\ \frac{1}{3}\ \frac{3}{8})$	$(-\frac{1}{3}\ \frac{1}{3}\ \frac{1}{8})$	$(-\frac{1}{3}\ -\frac{2}{3}\ \frac{1}{8})$
	QR59	$(\frac{2}{3}\ \frac{1}{3}\ \frac{1}{8})$	$(-\frac{1}{3}\ -\frac{2}{3}\ \frac{3}{8})$	$(\frac{2}{3}\ \frac{1}{3}\ \frac{3}{8})$	$(-\frac{1}{3}\ -\frac{2}{3}\ \frac{1}{8})$

The formation energy of a structure S containing (N_{Zr},N_H) atoms is

$$E_f(S) = E(S) - N_{Zr} \times E^0(\mathrm{Zr}) - N_H \times E^0(\mathrm{H}), \qquad (2)$$

where $E(S)$, $E^0(\mathrm{Zr})$, and $E^0(\mathrm{H})$ are obtained from *ab initio* calculations. The density-functional theory energies of the set of structures were determined with the Vienna *ab initio* simulation package (VASP) (Refs. 20 and 21) combining the use of ultrasoft pseudopotentials and plane-wave developments of the single-electron wave functions. The calculations were done with the GGA functional of Ref. 22. The reference energies are $E^0(\mathrm{Zr})=-8.403$ eV/atom and $E^0(\mathrm{H})=-3.884$ eV/atom, respectively, the cohesive energy of pure Zr and of isolated H in α Zr. All calculations included atomic and supercell shape relaxations, implying that the elastic interactions are at least partly accounted for by the CEs.

TABLE III. Number of invariant CEs for each R_n^p family for α H-Zr.

	Number of sites, p							
Range, n	1	2	3	4	5	6	7	8
2	1	5						
3	1	9	10					
4	1	17	162	328	334			
5	1	33	1790	46076	70219	84966	85026	
6	1	65	4964	346747	701180	912181	914401	914461

As regards assessing the quality of CEs, the simple root-mean-square criterion is well known to be useless, since it systematically selects the maximal CE and thus may not give a realistic picture of the prediction accuracy of CEs.[14,23] The cross-validation (CV) criterion[24] is frequently used as a measure of the prediction ability of a CE. The CV procedure divides the structure set into two subsets ("fit" and "prediction" structures), which, respectively, are used to fit the CE coefficients and calculate the prediction error. Different ways of constructing these sets have been proposed (for a discussion, see Ref. 25). Although more elaborate criteria have been recently developed for substitutional systems,[14] the present work, dealing with much less commonly investigated interstitial solid solutions, was carried out using the most frequent "leave-one-out" (LOO) CV criterion, a seemingly reasonable compromise of tractability and accuracy.

III. GROUND-STATE PROPERTIES

In cluster modeling of materials, the required optimal CEs not only should be efficient within the input data set, but also should correctly reproduce the whole ground-state properties. While some works have been performed using CEs constructed from the CV procedure associated with a nonevolutive structure set, it has been pointed out recently[14] that such an approach may lead to the unexpected presence of spurious ground states. Since fixing this deficiency requires an iterative update of the structure set (see below), it therefore seems useful to detail somewhat the present investigation devoted to the poorly known H-Zr. We will thus present in the next section the CEs obtained from a CV procedure applied with

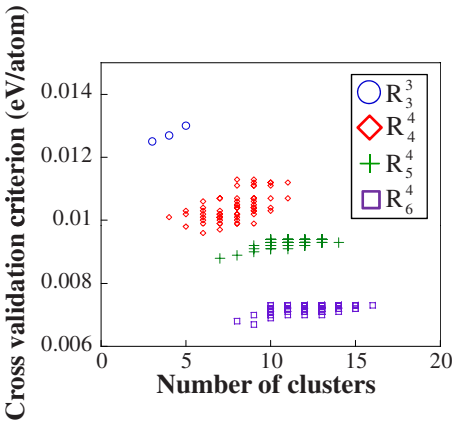

FIG. 2. (Color online) Comparison between the cross-validation minima of the R_n^4 cluster families, with the initial ensemble of 77 structures.

a fixed structure set, before turning to the role of the structure set enrichment.

A. Cross-validation fitting of CEs

Since in current CE methods, the structure set is a key ingredient, some words about it have to be given first. When tackling a new system, for which no such structures have been calculated with *ab initio* methods, this set requires to be constructed "from scratch," by proper choice of a sufficient number of (more or less) ordered compounds relevant for the system considered. In our case, an initial structure set was available, as already employed in previous investigations of the stable variants of ζ Zr_2H.[4] Although sufficient to deal with CEs included in R_3, this set had to be enriched in order to be also convenient for R_6, thus leading to a much larger (77) ensemble. Beginning the present α H-Zr study with this structure set composed of 77 elements (each containing at most 32 tetrahedral sites), Fig. 2 shows the results of the corresponding CV selection. The minimum zone of each R_n is rather shallow, suggesting that several ICEs might be equally favorable. Considering the trends associated with increasingly larger R_n families, it should be noted first that raising n improves the optimal CV score, which lies between 13 (R_3) and 7 (R_6) meV/atom.

As for the simplest family R_3, its CV criterion appears not to be improved by the addition of the TR3 triplet. In fact, the R_3 ICE which has the lowest CV criterion is particularly simple, since it contains only two clusters (besides the empty cluster ($\varnothing$) and the point ($\bullet$), implicit throughout): the pairs PR1 and PR2. This illustrates that the addition of a larger number of clusters does not necessarily improve the quality of prediction of CEs. Increasing the range up to the R_4 family (16 clusters), the ICE with the lowest CV criterion still offers moderate complexity, as it contains now 5 clusters: four pairs (PR1, PR2, PR3, PR4) and one triplet (TR44) (Fig. 3). Note that, although available, quadruplets are not selected in the optimal ICEs. Further increasing the range up to R_5 (30 clusters) confirms these clearcut trends, with an optimum of six clusters (PR1, PR2, PR3, PR5, TR3, TR52). It should be noted that the optimal CEs for R_4 and R_5 have close CV values ($\simeq$10 meV/atom), thus significantly improving the score obtained with R_3, at the only expense of a reasonably heavier modeling. Finally, the R_6 family (35 clusters) again shows an optimum with only eight clusters: five pairs (PR1, PR2, PR3, PR5, PR6) and three triplets (TR3, TR52, TR61), with a second noticeable jump of the CV score (7 meV/atom). The CV criterion therefore seems to confirm that the H-Zr energetics can be described quite precisely with light CE modeling. It also clearly points out the quadruplets as irrelevant cluster figures for H-Zr, suggesting that the energetics of the system has reached sufficient convergence with respect to the number of sites of clusters. Finally, it also appears unfavorable to consider CEs with more than $\sim$10 to 15 clusters.

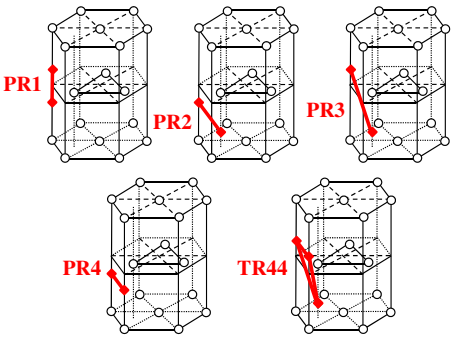

FIG. 3. (Color online) Relevant cluster figures for adequate CE description of the α H-Zr system.

The CV criterion is reputedly an efficient way to build CEs with real predictive ability. However, in order to reach a sufficient level of reliability, its use should be followed with a more thorough ground-state search. To this aim, an efficient procedure to perform an exhaustive symmetry-filtered direct enumeration of the configurational variants for a given superlattice has been proposed recently.[26] However, in order to lead to reasonable computational efforts, it should be applied to superlattices containing less than $\simeq$20 sites, whereas the systems considered in our work involve 32 tetrahedral sites (see below). An extrapolation of the data provided in Ref. 26 then indicates that the time required for a single ground-state search should exceed two months, which rules out this direct enumeration scheme for our purpose. The ground states of the H-Zr system were thus found by simulated annealing calculations using a MC Metropolis algorithm, the system being initially given a sufficient temperature ($T\simeq$500 K) and then slowly cooled down to 0 K. Because of the intricate coupling between CE and *ab initio* calculations, the latter being tractable only for a limited number of atoms (see Sec. III B), this MC ground-state determination was restricted to $2\times2\times2$ supercells, giving rise to 32 possible composition values. On-the-fly selection of the minimum energy configuration (rather than the last one) yielded $T=0$ K energy-composition profiles, the smoothness of which gives reasonable confidence in the efficiency of the search.

As displayed in Fig. 4(a), the $T=0$ K energy-composition curves for R_3 and R_4 both show a realistic behavior, following rather closely the convex hull of the *ab initio* data set on the whole Zr-ZrH_2 composition range. *Ab initio*—CE energy differences appear to be lower than 10 meV/atom, a reason-

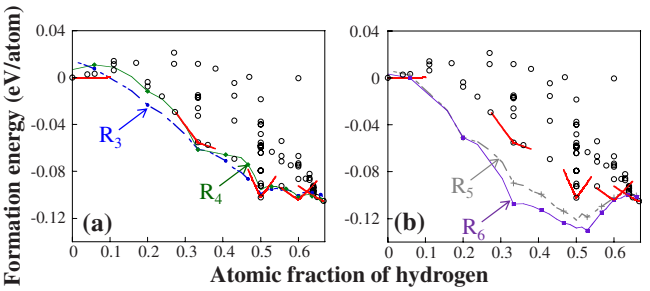

FIG. 4. (Color online) Ground-state properties of H-Zr for the optimal ICEs deduced from the cross-validation procedure applied to (a) R_3 and R_4 and (b) R_5 and R_6 (initial set of 77 structures, empty circles). Also shown (straight lines) are the low-temperature independent-defect slopes around several compounds with noticeable stoichiometries (see Sec. IV for details).

able accuracy with respect to the absolute values of the formation energies. More precisely, the best candidate seems to be the R_4 CE, which demonstrates an enhanced (although limited) trend to phase separation between Zr and ZrH. Whereas the behavior of R_3 in this composition range is almost linear (as would result from a CE limited to •), R_4 seems to favor the recently evidenced ζ hydride, with composition Zr_2H. Moreover, with a roughly zero slope for low H contents, R_4 accounts for the reduced H solubility in Zr, whereas the R_3 behavior is consistent with unexpectedly large amounts of diluted H at low temperature. It should be noted that the use of the canonical Monte Carlo algorithm allows to explore compositions which at equilibrium should lead to phase separation (hence inaccessible to grand canonical Monte Carlo). For $x_H > 1/2$, both R_3 and R_4 seem to identify a new (not contained in the *ab initio* structure set) stable compound with stoichiometry Zr_2H_3, this CE prediction being confirmed in the subsequent study (next section). An experimental confirmation of this feature may, however, be made difficult by the proximity (in terms of H content) of the equilibrium δ hydride with CaF_2 structure, the high stability of which may prevent such metastable compounds from appearing, even in a transient way. On the whole, R_4 seems a good candidate for further investigation of the thermodynamic properties of the H-Zr system. Although beyond the scope of the present analysis, it might also be instructive to refine the analysis, in order to identify which clusters specific to R_4 (PR3, PR4, TR44) are responsible for its improvement of the ground-state properties with respect to the simpler R_3 model.

Conversely, as illustrated by Fig. 4(b), the situation appears to be quite different when considering the ground-state properties predicted by R_5 and R_6, the energy-composition curves being strongly shifted down with respect to the *ab initio* data set. The R_5 and R_6 CEs yielded by the CV procedure thus appear inadequate for further modeling of H-Zr, since the structures obtained as most stable at each composition are in fact spurious ground states. This clearly indicates that the R_5 and R_6 CEs have not reached convergence with respect to the structure set, confirming that this issue is indeed critical in CE elaboration.[14] Before turning to this point, it should be stressed that R_4 and R_5 display quite distinct ground-state behaviors, whereas they were found close to each other in terms of mere CV criterion (cf. Fig. 2). This again emphasizes the limit of a pure CV approach for the determination of an optimal CE.

B. Autocoherent refinement of CEs

The previously mentioned deficiency of R_5 and R_6 suggests to carry out an autocoherence (AC) procedure, aimed at guaranteeing the convergence with respect to the set of structures, and iterated until a sufficient match is attained between the CE and *ab initio* ground-state energies. This AC procedure, similar to that employed with heuristic selection of CEs via genetic algorithms,[14] will be applied here in the framework of invariant CEs. One AC step practically consists in (i) adding to the structure set several selected spurious ground states corresponding to large *ab initio* CE-energy differences, (ii) performing again the complete (CV + ground state search) scheme. Although the previously obtained optimal R_3 and R_4 CEs seem to have reached the required convergence (as they apparently predict no spurious ground state), this important point deserves a more detailed checking. Therefore, while mainly aimed at improving the quality of the larger R_5 and R_6 CEs, AC will be performed consistently for all R_n families, including R_3 and R_4. The optimal ICEs yielded by AC are described in Table IV.

As any CE improvement should benefit first to the most remarkable (stable or strongly metastable) ordered compounds of the system, it is natural to consider in priority the relevant compositions. According to this rule, four structures were therefore selected at the first AC iteration. Firstly, the

TABLE IV. Clusters selected by the cross-validation criterion in the R_n^p family for each step of autocoherent procedure. Such a notation as PR1-5 means that (PR1, PR2, PR3, PR4, PR5) are included in the invariant CE.

AC step (number of structures)	R_3^3	R_4^4	R_5^4	R_6^4
Initial (77)	PR1-2	PR1-4	PR1-3 PR5	PR1-3 PR5-6
		TR44	TR3 TR52	TR3 TR52 TR61
First (81)	”	PR1-2	PR1-5 TR3	PR1-6 TR3
		PR4	TR52-4 QR59	TR52-4 QR59
Second (88)	”	”	PR1-5 TR3 TR41	PR1-6 TR3 TR41
			TR43-5 TR52 QR42 QR44	TR45 TR51-3 QR51 QR59

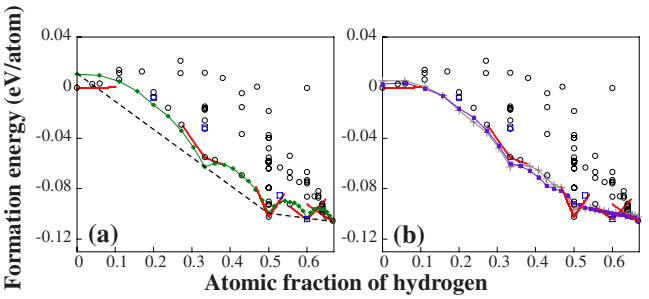

FIG. 5. (Color online) CE ground states of H-Zr at the first iteration of the autocoherent procedure (Sec. III B), (a) for R_4 (dashed line=CE convex hull indicating phase separation) and (b) for R_5 and R_6 (81 structure set, same symbols as in Fig. 4).

clear prediction by both R_3 and R_4 of a metastable Zr_2H_3 compound at the initial CV procedure required to take it into account. Moreover, as a secondary metastable compound was previously detected (see Fig. 4) by all CEs at Composition Zr_4H, the corresponding CE-favored structure was also added to the set. Thirdly, a satisfactory modeling of the properties of the recently identified Zr_2H hydride was required, and the erroneously stable structure at this composition was also introduced in the fitting set. Finally, the initial CV fitting seems to indicate that $x_H=1/2$ corresponds to a limit between two distinct composition zones, with an enhanced trend to ordering above this value [Fig. 4(a)], hence the importance of a correct energetic description around ZrH. As R_6 on the contrary favors H excess, checking of this surprising feature thus imposed to add to the set the off-stoichiometric Zr_8H_9 compound.

The new CV fitting with this set of 81 structures is found to have no effect on the optimal R_3 CE, which confirms that, within the framework of interactions limited to the third neighbor shell, the optimization scheme is indeed complete, pointing out a remarkably simple CE formed with only the first two tetrahedral pairs. It should be emphasized that such a simple modeling seems sufficient to reasonably reproduce the H-Zr bulk properties on the whole Zr-ZrH_2 composition domain (the short range of interactions may, however, be inadequate to describe sharp heterophase interfaces).

On the contrary, an important effect of the structure set enrichment is detected for the optimal CE of the R_4 family, the previously selected TR44 triplet being now discarded, as well as the third neighbor pair PR3. The new optimal R_4 ICE thus extends the optimum for R_3 by mere addition of the fourth neighbor pair PR4, again leading to a noticeably light modeling for H-Zr. The ground-state properties of this new R_4 optimum are displayed in Fig. 5(a). It confirms the trend to phase separation below $x_H=1/2$, as well as the privileged role of Zr_2H. On the whole, including PR4 improves the smoothness of the energy-composition profile in each two-phase zone. The trend to long-range ordering is increased above ZrH, with two-phase (metastable) fields limited by Zr_2H_3. The properties of the Zr(H) dilute solution, however, persistently appear to be difficult to describe accurately, as the CE-predicted energy of pure Zr is overestimated by more than 10 meV/atom. This failure may be, either due to the limited number of structures with low H content in the set (as it requires *ab initio* calculations on exceedingly large supercells), or a hint of longer-ranged interactions overlooked in the present modeling. Table V sums up the values of the formation energy coefficients of the R_3 and R_4 optimal CEs. The first two columns show that including (PR3, PR4, TR44) does not modify deeply the contribution of the common clusters. For R_4, using a 77-structure set clearly yields an oscillatory decaying influence of the pair coefficients, an effect seeked in the framework of MBCEs (Ref. 15) and arising spontaneously here. Moreover, increasing the structure set for R_4 mainly entails a moderate change for •, demonstrating the stability of the CE scheme.

TABLE V. Formation energy coefficients (eV) of the optimal ICEs of R_3 and R_4 (the latter both for the 77- and 81-structure sets).

Cluster	R_3	R_4 (77-structure)	R_4 (81-structure)
∅	−0.613	−0.641	−0.636
•	0.222	0.244	0.318
PR1	0.104	0.098	0.091
PR2	−0.075	−0.075	−0.076
PR3		0.049	
PR4		−0.001	−0.028
TR44		−0.053	

The situation is also strongly modified for R_5 and R_6: the enlarged structure set somewhat raises the complexity of the optimal CEs, the latter containing, respectively, 10 and 11 clusters. Another feature seems to be the emergence of a well-defined (the same for R_5 and R_6) fifth-neighbor quadruplet (QR59), whereas no such four-site figure (among 16 available, see Table I) was selected within R_4. As a refinement of the analysis (not performed here), the relevance of this QR59 selection (which may appear somewhat arbitrary) could be tested by identifying the clusters contained in the best CEs around the optimum. As expected, the resulting ground-state properties [Fig. 5(b)] of R_5 and R_6 optimal CEs are deeply modified, showing now more satisfactory energy-composition profiles. In particular, the behavior for $x_H<1/2$ is of comparable, or higher, accuracy than obtained from the R_4 ICE, with a much better description of the dilute Zr(H) solution. Since for low hydrogen amounts, the H atoms (or H clusters) necessarily interact via their elastic energy fields, the latter feature suggests that the multisite interactions included in R_5 and R_6 CEs are (partially) able to account for these long-range effects, at least in this domain of composition (this may, however, not be the case for higher H contents). On the other hand, R_5 and R_6 show a surprising behavior beyond ZrH, with almost linear profiles totally overlooking specific ordering in the intermediate Zr_2H_3 compound. This constitutes the main discrepancy between the simple pair CEs of R_3 and R_4, and the longer-ranged multisite ones of R_5 and R_6. Due to the importance of this issue for a proper choice of the H-Zr energy model, we will return to this CE comparison in the next section.

As the various models obtained at this stage no longer show erroneous ground states at characteristic compositions, this probably means that the CE convergence reached with

the 81-structure set is sufficient. In order to check this point, one more AC step was performed, adding several (7) new compounds with various compositions between pure Zr and ZrH. The energy-composition profiles deduced from this 88-structure set yields the same R_4 optimum previously, confirming that the convergence is reached for this family. As for R_5 and R_6, on the contrary, this second AC iteration surprisingly entails the emergence of new spurious ground states on the whole composition domain. This erroneous behavior for R_5 and R_6 could be corrected again by further iterations of AC (not shown for brevity), however, with a persistent "oscillating" behavior (erroneous prediction—correction) that may be related to the LOO CV criterion adopted, since the latter is known to favor artificial complexity of the CEs.[25] This point would deserve further investigation, for instance, by employing a "leave many out" variant of the CV criterion, as suggested in Ref. 25. Anyway, this remark does not invalidate the previous conclusions about the optimal CEs obtained at the initial and first AC steps.

C. Cluster expansions and point defects in Zr_xH_y

The foregoing analysis was intended to provide a thorough insight of the effect of the various parameters entering the elaboration of a CE energy model. The R_n^p adopted hierarchy revealed two quite distinct ground-state behaviors (R_3-R_4 vs R_5-R_6) related to the complexity of the optimal ICEs. More extensive investigations (including thermodynamic calculations, interface studies,…) would be beneficial, in order to discriminate between these two types of models. Leaving these investigations for future work, we will go on here with low-temperature properties, confronting the previous CE ground-state predictions with those deduced from an independent-point-defect approach (IPDA), much easier to handle than CEs, and successively applied to a few ordered compounds relevant for H-Zr. The basic quantities required to perform an IPDA analysis, namely, the grand canonical defect energies (see, for instance, Ref. 27), were calculated using the same *ab initio* method (VASP) as employed to get the energies of the structure set. As the present CE analysis mainly points out the local (meta) stability of three structures, namely, ZrH, ζZr_2H, and Zr_2H_3, the properties of these ordered compounds around stoichiometry can therefore be analyzed in an IPDA framework. Our goal here is not to study the point defect properties inferred from the above CE modeling, but rather to draw the reader's attention on the link between CE and IPDA, since both approaches usually form the subject of separate publications although they address quite close issues. In spite of its simplicity, IPDA is exact in the limiting case of low departures from stoichiometry (δx) and $T \to 0$ K, and can therefore be regarded as a reference point for the behavior of CEs around ordered compounds, both approaches being expected to yield identical results. Discrepancies may thus be the hint, either of defect clustering (probably an exceptional case in the low $(\delta x, T)$ domain, dealt with by IPDA refinement—see below for Zr_2H_3) or of the inadequacy of the CE considered. In the present H-Zr system, for which several CEs of seemingly close merits could be built, IPDA may therefore help to discriminate between these CEs.

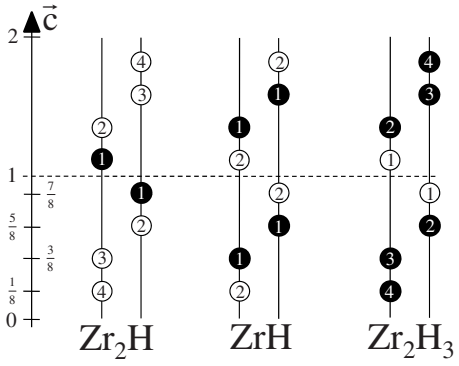

FIG. 6. Tetrahedral site occupancies of the structures used for independent-defect calculations (full circle=H, empty circle =unoccupied site).

In this scheme, the following point defects were considered (Fig. 6): (i) for ZrH, (V_1, H_2) (H vacancy on site 1 and interstitial H on site 2), (ii) for Zr_2H, (V_1, H_2, H_3, H_4) (vacancy on site 1, interstitial H on sites 2, 3, and 4), (iii) for Zr_2H_3, (H_1, V_2, V_3, V_4) (interstitial H on site 1, vacancy on sites 2, 3, and 4), namely, two- and four-defect modelings. A low-temperature calculation of the IPDA free energy of a given ordered compound yields roughly straight lines which provide information (local slopes of the energy-composition curves) that can be compared to the previous CE modelings. For completeness, dilute Zr(H) and substoichiometric ZrH_2 were also modeled along the same lines, and the local IPDA behaviors in the five relevant composition ranges are displayed in Figs. 4 and 5 (it can be noticed that the slopes calculated with the IPDA analysis closely follow the *ab initio* data). The comparison with the CE behavior shows that R_3 and R_4 should probably be preferred, since they globally yield better free energy derivatives (chemical potentials) of the main ordered phases around stoichiometry. Admittedly, R_5 and R_6 CEs, after iteration 1 of AC, provide for ζ Zr_2H (and also for the dilute H solution) a picture very consistent with IPDA, but their behavior is probably not satisfactory beyond $x_H = 1/2$, where IPDA confirms the strong ordering tendency already deduced from R_3 and R_4 CEs, thus invalidating R_5 and R_6.

Due to its key position (at the heart of the composition zone where CE discrepancies are prominent), the compound Zr_2H_3 must be investigated in detail. In particular, IPDA can be considered as a valid low-T, low δx description only when possible "structural" complex defects are taken into account.[28] Since the latter IPDA analysis was confined to single-site point defects, its stability should be tested with respect to the inclusion of double defects. Such a test was performed for Zr_2H_3, by insertion into the IPDA formalism of the six possible first double defects, resulting in an improved ten-defect IPDA model. The corrected IPDA free energy is not modified with respect to the previous one (including only single defects) below $T \simeq 500$ K, which reinforces the previous conclusion of strong ordering around Zr_2H_3. This also means that the latter compound should not be prone to "structural" (low-T) complexes. It is worth noticing the agreement between the CE and IPDA approaches, respectively, having a global or local character (with respect to

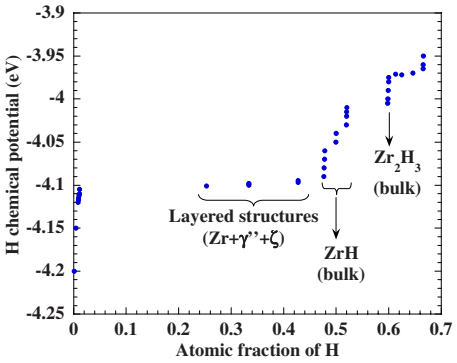

FIG. 7. (Color online) Grand canonical Monte Carlo calculation at $T=500$ K, using the optimal R_4 CE and a $12\times12\times12$ supercell (6912 sites).

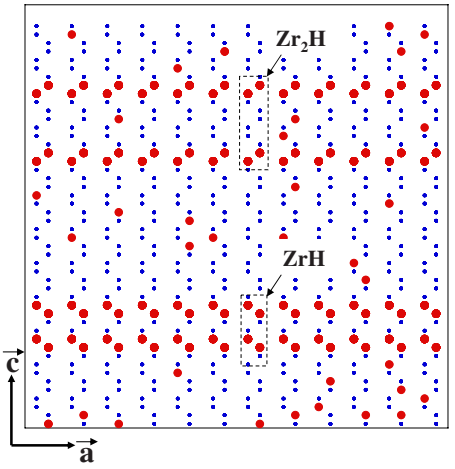

FIG. 8. (Color online) Typical $\zeta/\alpha/\gamma''$ lamellar H arrangement obtained at 500 K for a Monte Carlo simulation (see text for details), the global composition of the system being Zr_3H (H atoms and empty tetrahedral sites are represented by full circles and dots, respectively).

composition). This reinforces a major conclusion of the present analysis, namely, that the R_4 CE presented above should probably be preferred for further thermodynamic modeling of α H-Zr.

IV. DISCUSSION: HYDRIDE PRECIPITATION

In the context of the present work, it is interesting to tackle the practically important issue of hydride precipitation in H-Zr. Although at equilibrium only the incoherent δ phase Zr_2H_{1-x} should form, the question arises as to which mechanisms do favor the emergence of coherent ZrH (Ref. 5) or Zr_2H (Ref. 4) precipitates, all the more since the previous analysis indicates that, in the $T=0$ K limit, both types of particles should have similar stabilities. The above CE modeling was therefore used to get preliminary information about the expected precipitation sequence of these hydrides. For this purpose, we performed finite-temperature Monte Carlo calculations within a grand canonical scheme, allowing for H-vacancy "transmutations" in the interstitial tetrahedral sublattice of a 6912-site system, in order to overcome the possible limitations induced by the previously used $2\times2\times2$ supercell. The H chemical potential μ_H was varied over a sufficient range, in order to explore the whole $x_H\in[0;2/3]$ composition range, the μ_H increment being reduced down to 1 meV when necessary. For each μ_H value, the system was first equilibrated using a 5×10^6-step run (in order to ensure a sufficient $\sim10^3$ MC steps/site of supercell), and the average x_H was calculated with a second run of similar size. The evolution of the system being sometimes found to proceed by sudden composition changes (associated with overall layered morphologies—see below), the convergence in these cases was checked through much longer (2×10^8 MC steps) runs, in order to eliminate "spurious" (nonphysical) metastable states.

Figure 7 shows the corresponding $\mu_H(x_H)$ dependence at $T=500$ K. At this temperature, the solubility limit of H reaches $\sim1\%$, a result reasonably agreeing with the experimental estimations[3] of $\sim0.2\%$. Beyond this limit, the system directly switches towards (γ') ZrH_{1-x} ($x_H\simeq42\%$), which thus appears as the first ordered compound with significant bulk stability. For a narrow range of μ_H, the α-γ'' two-phase domain is partially occupied by layered structures with global compositions Zr_3H and Zr_2H. However, these structures are not single-phase compounds, but gradually denser pile ups of (0001) H planes, the relative position of these planes inducing layered arrangements of locally α, ζ, and γ'' character. Below $x_H=0.5$, the observed lamellar microstructures (Fig. 8) may be described in terms of stacking of double H planes ("biplanes") along the c axis, as depicted previously by Fig. 6. It should be emphasized that ζZr_2H is not found to form spontaneously, which may be a hint (admitting, from Ref. 4, the existence of ζ particles in bulk form) that the stability of ζ depends on weak and long-range (elastic) interactions, which are not accounted for by the present short-range CE model. These low interactions should be responsible for the arrangements of the aforementioned H biplanes, possibly contributing to the relative stability of γ'' and ζ. However, the good agreement between the CE and *ab initio* results (Fig. 5) suggests that the present modeling grasps the essential part of the energetics of the H-Zr system, consisting in strong interactions within the basal plane and leading to biplane formation. For larger H contents, the finite-temperature simulation also confirms the stability of a bulk phase with composition Zr_2H_3, having the characteristics of a strongly ordered compound and showing a dissymmetric behavior (off stoichiometry only for H excess). It should be noted that the possible existence of Zr_2H_3 is a prediction of the CE modeling, which would be fruitfully confronted with experimental measurements of the composition within hydrides.

As mentioned above, the equilibrium δ (CaF_2) Zr_2H_{1-x} hydrides are believed to form from γ (fct) ZrH particles. The efforts devoted to understand the formation of these γ particles gave rise to two distinct interpretations, depending on the composition of the preexisting germs which undergo the hcp$\rightarrow$fct dislocation-induced transformation. Whereas the first hypothesis[5] admitted for these germs a composition x_H nearly 0.5, recent experiments seem to indicate that a much lower H content is required, with the introduction of a new ζ

compound.[4] Our work points out the possibility of strong fluctuations of compositions (between Zr_2H and ZrH) in these germs, which, however, are described in all cases by stackings of *H* biplanes. Another noticeable point concerns the strong stability of Zr_2H_3, which might be closely related to the appearance of ϵ precipitates, in a way similar to the formation of γ from γ' or ζ. More precisely, a $Zr_2H \rightarrow \epsilon$ sequence might constitute an alternative to the usually proposed $\delta \rightarrow \epsilon$ mechanism.

V. CONCLUSION

In order to shed light on the physical processes of hydride precipitation in zirconium, the aim of the present work was to model the coherent α H-Zr system by cluster methods. This study evidences the existence of several metastable structures in the composition domain $x_H = 0.2-0.65$, which suggests that the formation of stable (δ) or metastable (γ) hydrides is triggered by the emergence of coherent phases, as also shown experimentally. In spite of this wealth of configurations, the most adequate cluster expansions show a remarkable simplicity, implying only a few pairs, and leading to an enhanced stability for layered structures along the *c* axis (*H* biplanes). The main energetic properties of the α H-Zr system can thus be conveniently described by short-ranged interactions. However, obtaining more subtle information about the actual arrangement of (0001) *H* biplanes requires to refine the energy model by including long-range interactions parallel to *c*, a feature that may be fruitfully described with mixed-basis cluster expansions.

*laurent.holliger@ed.univ-lille1.fr
†alexandre.legris@univ-lille1.fr
‡Author to whom correspondence should be addressed. remy.besson@univ-lille1.fr

[1] Y. Fukai, *The Metal-Hydrogen System* (Springer-Verlag, Berlin, 1993).
[2] A. Aladjem, Solid State Phenom. **49-50**, 281 (1996).
[3] E. Zuzek, J. Abriata, A. San-Martin, and F. Manchester, Bull. Alloy Phase Diagrams **11**, 385 (1990).
[4] Z. Zhao, J.-P. Morniroli, A. Legris, Y. Khin, L. Legras, and M. Blat-Yriex, J. Microsc. **232**, 410 (2008).
[5] G. Carpenter, Acta Metall. **26**, 1225 (1978).
[6] J. M. Sanchez, F. Ducastelle, and D. Gratias, Physica A **128**, 334 (1984).
[7] F. Ducastelle, *Order and Phase Stability in Alloys* (Elsevier Science, New York, 1991).
[8] V. Vaithyanathan, C. Wolverton, and L. Q. Chen, Phys. Rev. Lett. **88**, 125503 (2002).
[9] N. A. Zarkevich and D. D. Johnson, Phys. Rev. B **67**, 064104 (2003).
[10] P. Narang, G. Paul, and K. Taylor, J. Less-Common Met. **56**, 125 (1977).
[11] A. Seko, A. Togo, F. Oba, and I. Tanaka, Phys. Rev. Lett. **100**, 045702 (2008).
[12] M. H. F. Sluiter and Y. Kawazoe, Phys. Rev. B **71**, 212201 (2005).
[13] Z. W. Lu, S.-H. Wei, A. Zunger, S. Frota-Pessoa, and L. G. Ferreira, Phys. Rev. B **44**, 512 (1991).
[14] S. V. Barabash, V. Blum, S. Müller, and A. Zunger, Phys. Rev. B **74**, 035108 (2006).
[15] D. B. Laks, L. G. Ferreira, S. Froyen, and A. Zunger, Phys. Rev. B **46**, 12587 (1992).
[16] S. Müller, L.-W. Wang, A. Zunger, and C. Wolverton, Phys. Rev. B **60**, 16448 (1999).
[17] M. H. F. Sluiter, C. Colinet, and A. Pasturel, Phys. Rev. B **73**, 174204 (2006).
[18] V. Blum, G. L. W. Hart, M. J. Walorski, and A. Zunger, Phys. Rev. B **72**, 165113 (2005).
[19] N. A. Zarkevich and D. D. Johnson, Phys. Rev. Lett. **92**, 255702 (2004).
[20] G. Kresse and J. Furthmüller, Phys. Rev. B **54**, 11169 (1996).
[21] G. Kresse and J. Furthmüller, Comput. Mater. Sci. **6**, 15 (1996).
[22] J. P. Perdew, J. A. Chevary, S. H. Vosko, K. A. Jackson, M. R. Pederson, D. J. Singh, and C. Fiolhais, Phys. Rev. B **46**, 6671 (1992).
[23] L. G. Ferreira, M. Marques, and L. K. Teles, Phys. Rev. B **74**, 075324 (2006).
[24] M. H. F. Sluiter, Y. Watanabe, D. de Fontaine, and Y. Kawazoe, Phys. Rev. B **53**, 6137 (1996).
[25] V. Blum and A. Zunger, Phys. Rev. B **70**, 155108 (2004).
[26] G. L. W. Hart and R. W. Forcade, Phys. Rev. B **77**, 224115 (2008).
[27] B. Meyer and M. Fahnle, Phys. Rev. B **59**, 6072 (1999).
[28] R. Besson, A. Legris, and J. Morillo, Phys. Rev. B **74**, 094103 (2006).